Defence Science Journal, Vol. 75, No. 4, July 2025, pp. 433-443, DOI : 10.14429/dsj.20366

Design and Development of an Electronically Controlled Polarization Agile Slotted Waveguide Array Antenna

Mandar Chakrabarti[#,*], Abir Chattopadhyay[#], Malay Gangopadhyaya[#], Ayan Chatterjee[#] and Kabita Purkait[$]

[#]*Department of ECE, Institute of Engineering and Management, University of Engineering and Management, Kolkata - 700 160, India*

[$]*Department of ECE, Kalyani Government Engineering College, Kalyani, Nadia - 741 235, India*

[*]*E-mail: mandarc02@gmail.com*

ABSTRACT

This paper presents a new design for a polarization agile slotted waveguide array antenna that can dynamically switch between four polarization states: Vertical Polarization (VP), Horizontal Polarization (HP), Right-Handed Circular Polarization (RHCP), and Left-Handed Circular Polarization (LHCP) via electronic control of the antenna's power feed. The multi-layered antenna uses a custom-designed patch array as an actively regulated polarizing grid placed over the slotted waveguides. A 1-by-4 antenna array operating at 2.5 GHz was designed, fabricated, and tested to ensure its effectiveness. Results show realized gains of 13.84 dBi (VP), 11.81 dBi (HP), 11.86 dBi (RHCP), and 11.66 dBi (LHCP), with an axial ratio of 1.1dB and impedance bandwidth of 32 MHz. This architecture provides greater flexibility and performance over traditional designs. It is also suitable for modern radar and remote sensing systems due to its creative design and easy integration with advanced polarimetry algorithms.

Keywords: Slotted waveguide array antenna; Polarization diversity; Circular polarization; Linear polarization; Remote sensing antenna

NOMENCLATURE

λ_0 : Free space wavelength
λ_g : Guided wavelength
ε_r : Relative permittivity
tan δ : Loss tangent

1. INTRODUCTION

Reconfigurable antennas, capable of dynamically altering their radiating characteristics or operating frequency, have transformed modern radar, remote sensing, and wireless communication systems. Contemporary radar systems utilize multiple frequencies and polarization states to mitigate electromagnetic interference and multipath propagation error challenges.

Polarimetry algorithms are crucial for data interpretation in modern radar and remote sensing systems, significantly improving resolution by resolving fine target details[1-3]. By using polarimetry algorithms, modern remote sensing systems can enhance target identification and reduce cross-polarization interference and multipath issues, thereby improving signal reception and reducing fading effects[4-5]. Polarimetry works by analyzing the polarization state of the backscattered electromagnetic wave after it interacts with the target object. These algorithms process data from multiple polarization states—such as Vertical Polarization (VP), Horizontal Polarization (HP), Right-Handed Circular Polarization (RHCP), and Left-Handed Circular Polarization (LHCP)—to extract detailed information about the target's physical and structural properties. Polarimetric algorithms such as the Cloude-Pottier decomposition, Freeman-Durden decomposition, and polarimetric target classification models enable advanced image interpretation and target discrimination, which can enhance the detection of features such as surface roughness, material composition, and geometric structure.

Since polarimetry algorithms process data from multiple polarization states, the implementation of polarimetry techniques requires an antenna that can radiate or detect various polarization states, both linear and circular polarization. Waveguide slot array antennas are popular in radar and remote sensing applications due to their lightweight, ease of manufacture, high mechanical tolerances, efficiency, and power handling capabilities, especially in airborne or spaceborne platforms[6]. These antennas typically produce strong linearly polarized radiation patterns with good cross-polar isolation. However, achieving electronically adjustable polarization diversity in slotted waveguide arrays remains challenging.

This paper proposes a novel design for an electronically controlled, polarization-agile waveguide slot array antenna. A comprehensive literature review categorizes existing techniques for achieving multiple polarization states or even circular polarization in slotted waveguide array antennas into three groups:

- **Interleaving Technique**[7-10]: This method employs a planar array of waveguides with slots cut alternately either into the waveguide's broad wall or into the narrow wall. This technique can also produce multiple polarization states by switching the power supply points.[11] However, it suffers

Received : 15 July 2024, Revised : 28 March 2025
Accepted : 24 April 2025, Online published : 26 June 2025

from aperture obstruction and mutual coupling between waveguides, reducing performance and increasing cross-polarization levels.

- **Slot Configuration Modification**: This method uses compound[12-14] or crossed slots[15,16] in a traveling wave arrangement to create circular polarization. Multiple polarization states can also be achieved by providing power feeds from either end of the antenna structure.[17] This method often results in large grating lobes due to higher inter-element spacing, reducing antenna gain and efficiency.
- **Polarizing Grid Technique**: This method uses a polarizing grid of metallic cavities[18-22] positioned above the radiating slots to create circular polarization. While it is effective, the metallic cavities increase the antenna height and significantly add to its weight, rendering them unsuitable for airborne or spaceborne deployment. An alternative variation of this technique substitutes the metallic cavities with a simple layer of printed dipoles, which serve as a polarizing grid[23-25]. Printed dipoles add structural complexity that introduces additional losses, reducing efficiency.

The polarizing grid method generates better circular polarization than interleaving or slot geometry modification methods, but cannot produce multiple polarization states. This investigation proposes a novel method to achieve electronic switching between four polarization states: horizontal linear, vertical linear, right-handed circular, and left-handed circular polarization. The proposed antenna is multi-layered, featuring an actively controlled microstrip patch array mounted on top of the slotted waveguide array as the polarizing grid, tuned for S-Band radar applications at 2.5 GHz.

Subsequent sections provide detailed insights into the design and working principle of this novel method. A 1x4 antenna array has also been fabricated and tested to validate the design. Additionally, the performance of the proposed antenna is compared with parasitic dipole-loaded slot arrays to highlight improvements.

2. DESIGN OF PROPOSED POLARIZATION AGILE ANTENNA

To enable polarization state changes, this paper proposes to replace the passive parasitic dipole layer with an actively controlled polarizing layer. The new design features an actively controlled microstrip patch array placed directly on top of the waveguide slot array, allowing electronic control over polarization. Figure 1(a) and Fig. 1(b) show the layer-by-layer isometric figure and the final fabricated model of the proposed antenna.

The proposed antenna, shown in Fig. 1(a), features a two-layer design. The bottom layer is an aluminum WR340 slotted waveguide array with a cross-sectional dimension of 86.36 mm × 43.18 mm

The resonant length and offset distance of the radiating slots are calculated using Eqn. (1) and Eqn. (2), respectively[26-29].

$$l = [0.21034\left(\tfrac{1}{N}\right)^4 - 0.338065\left(\tfrac{1}{N}\right)^3 + 0.12712\left(\tfrac{1}{N}\right)^2 + 0.034433\left(\tfrac{1}{N}\right) + 0.48253]\lambda_0 \quad (1)$$

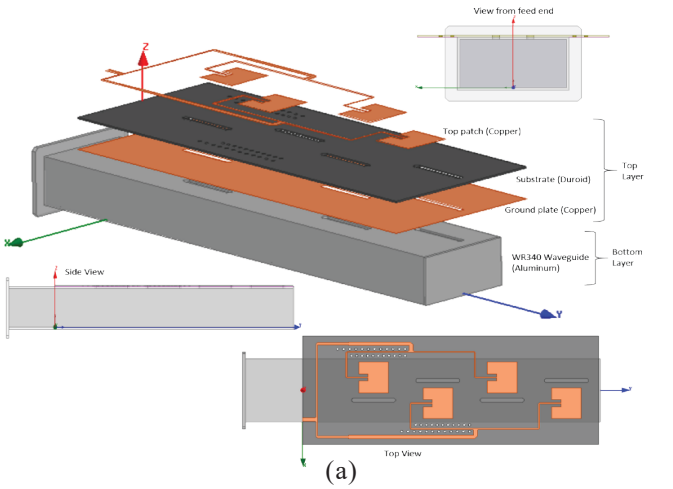

(a)

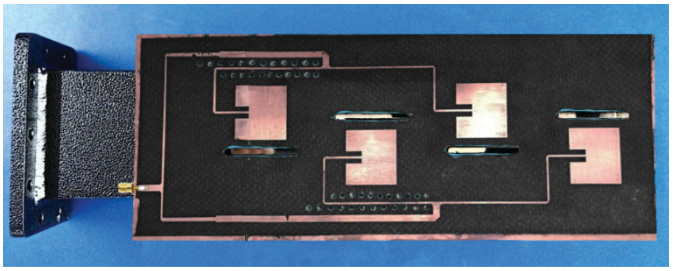

(b)

Figure 1. (a) Layer-by-layer isometric figure of the proposed antenna; and (b) Photograph of the fabricated model of the same antenna.

$$\frac{G_{slot}}{G_{w/g}} = \left[2.09\frac{\lambda_g}{\lambda_0}\frac{a}{b}\left(\cos\left(\frac{0.464\pi\lambda_0}{\lambda_g}\right) - \cos(0.464\pi)\right)^2\right]\sin^2\frac{\pi d}{a} \quad (2)$$

where, '$G_{slot}/G_{w/g}$' = 1/N and 'N' is the size of the array, 'l' is slot length, 'l_0' is free space wavelength, 'l_g' is guided wavelength, 'a' is broad-wall dimension of waveguide, 'b' is narrow-wall dimension of waveguide, 'd' is the slot offset, '$G_{slot}/G_{w/g}$' refers to the normalized conductance of each slots. The first slot element is placed at a distance of lg/4 from the short-circuit end of the waveguide, and inter-element spacing between the rest of the slot elements has been maintained at lg/2 to ensure the non-occurrence of beam tilting.[30] Optimal performance was achieved from slot length and offset values of 62 mm and 14 mm, respectively.

The upper layer is an actively controlled microstrip patch array, using a 1.6 mm thick Rogers RT/Duroid 5880 substrate (ε_r = 2.2, tan δ = 0.0009). Slots are cut in the substrate aligned with the waveguide slots below. Each patch element is positioned adjacent to the slots with a 28 mm slot-to-patch lateral distance (determined through detailed parametric analysis as given in Section 4.3), symmetrically alternating around the waveguide's centerline. Therefore, the inter-element spacing between the patch elements is also maintained at $\lambda_g/2$.

A specially crafted corporate power feed network powers the patch elements, ensuring proper phase matching. The surface current distribution on each patch element is orthogonal to the current distribution across the narrow walls of the slots (as shown in Fig. 2), with the distance between the slot and the patch optimized for phase quadrature. Each patch element is designed using standard design Eqn. to resonate at

2.5 GHz. All parameters are optimized on Ansoft HFSS using the pattern search optimizer. Table 1 details all relevant design parameters.

Table 1. Design parameters of the proposed reconfigurable slotted waveguide array antenna

Waveguide parameters (in mm)		Power divider parameters (in mm)		Patch parameters (in mm)	
Broadwall dimension (a)	86.36	MS Line width (50 ohms)	4.93	Patch height	39.6
Narrow wall dimension (b)	43.18	MS Line width (70.7 ohms)	2.828	Patch width	43.9
Waveguide length (L)	457.93	MS Line width (100 ohms)	1.434	Feed inset	10.4
Waveguide wall thickness (t)	2	Length of each arm	140.7		
Slot length (s_l)	57	Mitre bend 1	3.69	Slot-patch distance	28
Slot offset (s_off)	14	Mitre bend 2	1.44		

The designed antenna can electronically switch between four polarization states: Horizontal Linear Polarization, Vertical Linear Polarization, Right-Handed Circular Polarization, and Left-Handed Circular Polarization. This is possible through independent control over the power feed of the two layers of the antenna. For the present study, the design of an electronic switching network has been kept beyond the purview of the study. For experimental validation, manual switching was used. The use of an independent, actively controlled polarization grid provides an added degree of freedom. If the polarizing grid is turned off, horizontal linear polarization can be achieved. In essence, it is similar to the presence of only the conventional waveguide slot array without the presence of a polarizer. Vice versa, if the polarizing grid is excited alone, keeping the lower layer turned off, it acts like a standard microstrip patch antenna array. The surface current distribution aligns with the width of the rectangular patch, generating vertical linear polarization.

Exciting both layers simultaneously induces two orthogonal current distributions on the antenna's radiating surface, resulting in circular polarization. The horizontal distance between the slot and the patch is optimized to achieve the desired phase quadrature. When both layers are powered in phase, right-handed circular polarization is produced. However, if the phase of either the polarizing grid or the waveguide slot array is shifted by 180°, left-handed circular polarization is produced.

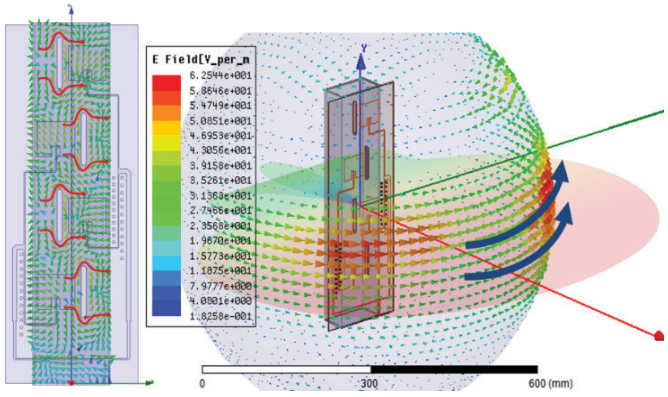

Lower layer: Switched ON; Upper Layer: Switched OFF
(a)

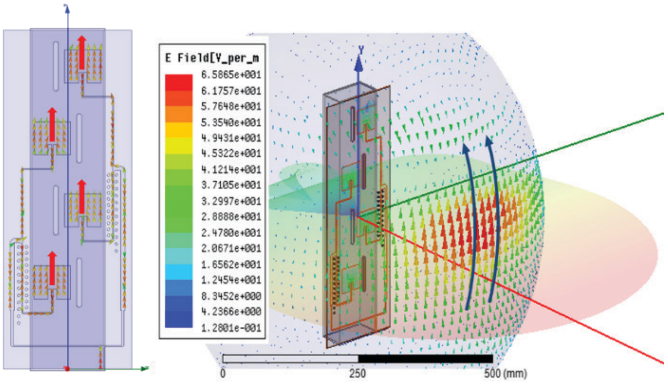

Lower layer: Switched OFF; Upper Layer: Switched ON
(b)

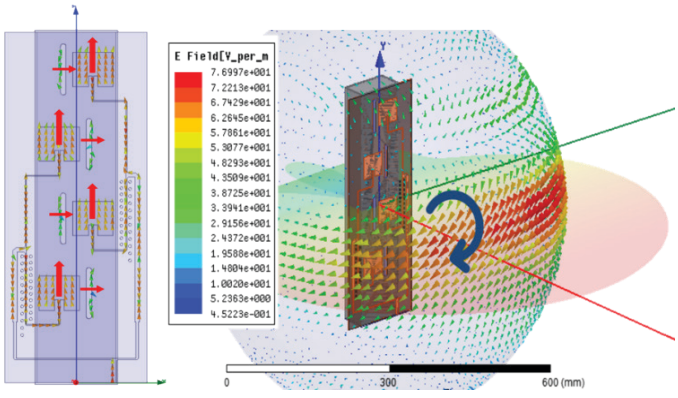

Lower layer: Switched ON; Upper Layer: Switched ON (same phase)
(c)

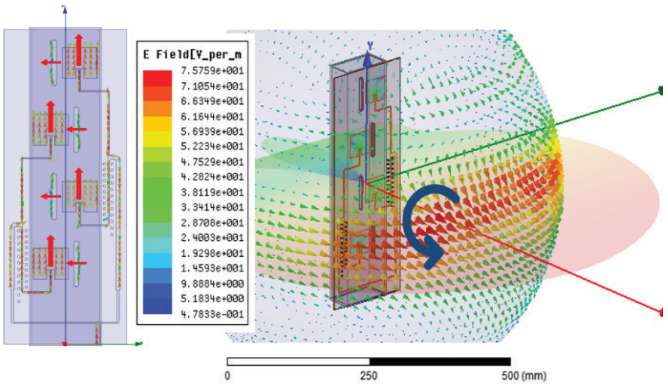

Lower layer: Switched ON; Upper Layer: Switched ON (opposite phase)
(d)

Figure 2. Surface Current vectors (radiating face) and electric field vectors (far-field region) of the antenna observations for (a) Horizontal linear polarization,; (b) Vertical linear polarization; (c) Right-handed circular polarization; and (d) Left-handed circular polarization (results considered at 2.5 GHz).

3. SIMULATED & MEASURED RESULTS OF THE PROPOSED ANTENNA

3.1 Radiation Characteristics

Radiation characteristics of the proposed antenna at each polarization state are examined in detail and presented in this section.

Current distribution vectors on the radiating surface of the antenna, along with electric field vectors at the far-field region, are observed for all four polarization states and are shown here. Figure 2(a) depicts horizontal linear polarization. Figure 2(b) depicts vertical linear polarization. Right-handed circular polarization is shown in Fig. 2(c), and left-handed circular polarization is shown in Fig. 2(d).

Notably, the electric field distribution in Fig. 2(a) is predominantly aligned in the x-direction, indicating horizontal linear polarization. In Fig. 2(b), the electric field distribution is primarily oriented in the y-direction, indicating Vertical Linear Polarization. Figures 2(c) and Fig. 2(d) show that when both layers are activated simultaneously, the electric field vectors in the far field area lose linearity and exhibit a circular tendency, indicating Circular Polarization. RHCP or LHCP is defined by whether the two layers are in the same or opposite phase.

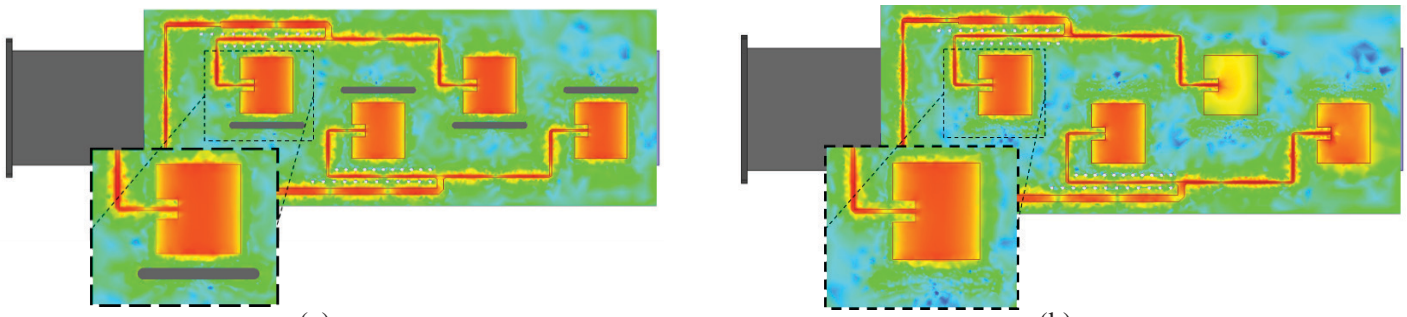

(a) (b)

Figure 3. Surface Current distribution on radiating face of the antenna when (a) slots and patch are present in near vicinity; and (b) with slots removed.

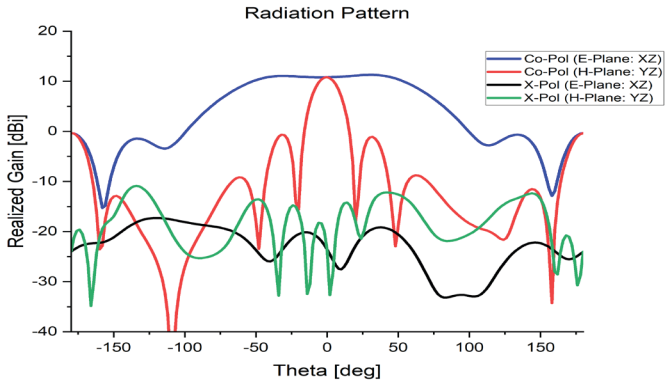

Maximum gain: 11.75 dBi; Cross polar isolation: 34.82 dB

(a)

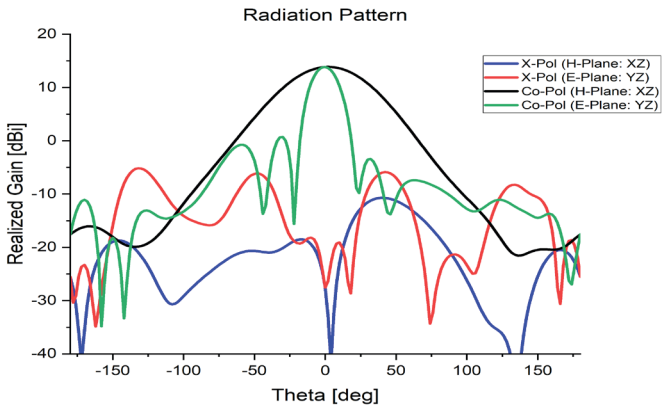

Maximum Gain: 13.65 dBi; Cross polar isolation: 40.12 dB

(b)

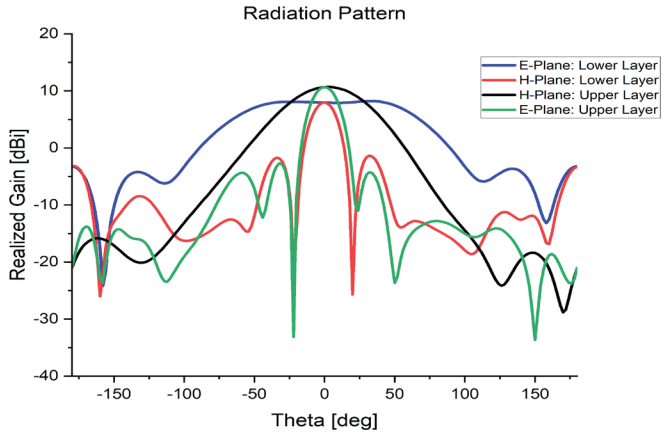

Maximum Gain: 11.51 dBi

(c)

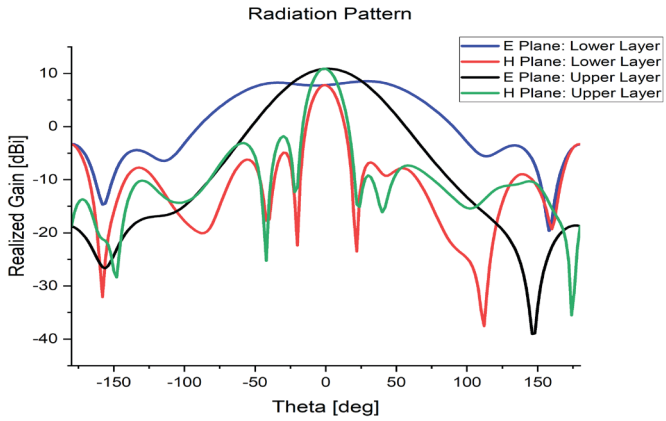

Maximum Gain: 11.45 dBi

(d)

Figure 4. Simulated Radiation Pattern graphs of the proposed antenna for (a) Horizontal linear polarization; (b) Vertical linear polarization; (c) Right-handed circular polarization; and (d) Left-handed circular polarization (All measurements taken at a design frequency of 2.5 GHz).

As shown in Section 2, slots are cut in the Duriod substrate aligned with the radiating slots of the waveguide below. Since the patch elements are placed close to the slots, there remains a possibility of edge effects between the slot and the patch, leading to a distortion of the radiation pattern due to uneven distribution of surface currents. This has been confirmed through simulation by observing the change in surface current distribution on the radiating face of the substrate by removing the slots. Observations show insignificant changes in this case. Figure 3(a) shows the surface current distribution when both the patch and slot are present, and Fig. 3(b) shows the surface current distribution with slots removed and no other changes.

Radiation patterns of all four polarization states are inspected as well. Figure 4(a) depicts horizontal linear polarization. Figure 4(b) depicts vertical linear polarization. Right-handed circular polarization is shown in Fig. 4(c) and left-handed circular polarization is shown in Fig. 4(d).

The optimal axial ratio value for circular polarization is 1 dB. However, for realistic designs, values of less than 3 dB are completely acceptable. Figure 5(a) shows the axial ratio values for each polarization state at the design frequency of 2.5 GHz. As expected, horizontal and vertical linear polarization states have very high axial ratios of around 40 dB. Right-handed circular polarization and left-handed circular polarization have low axial ratios of around 1.8 dB and 1.2 dB, respectively. When dealing with circular polarization, it is essential to monitor the frequency range over which circular polarization is preserved.

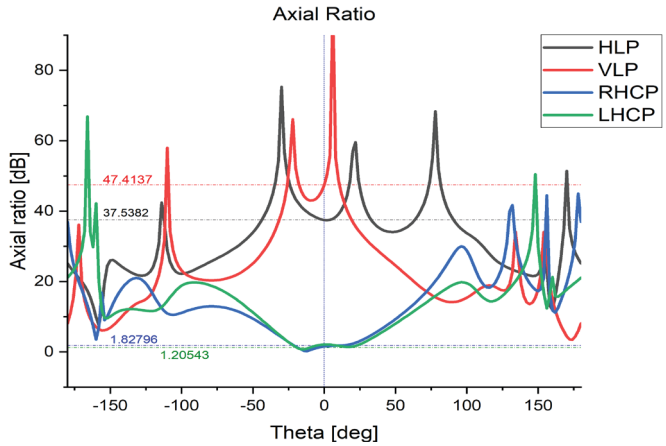

Figure 5. (a) Simulated Axial Ratio graphs of the 4 polarization states of the proposed antenna; and (b) Axial ratio bandwidth at the two circular polarization states of the proposed antenna.

Furthermore, Fig. 6 (a) indicates that the circular polarization achieved when both layers are excited in the same phase is indeed Right-Handed Circular Polarization. Similarly, when both layers are excited in opposite phase, Fig. 6(b) indicates that Left-Handed Circular Polarization is generated.

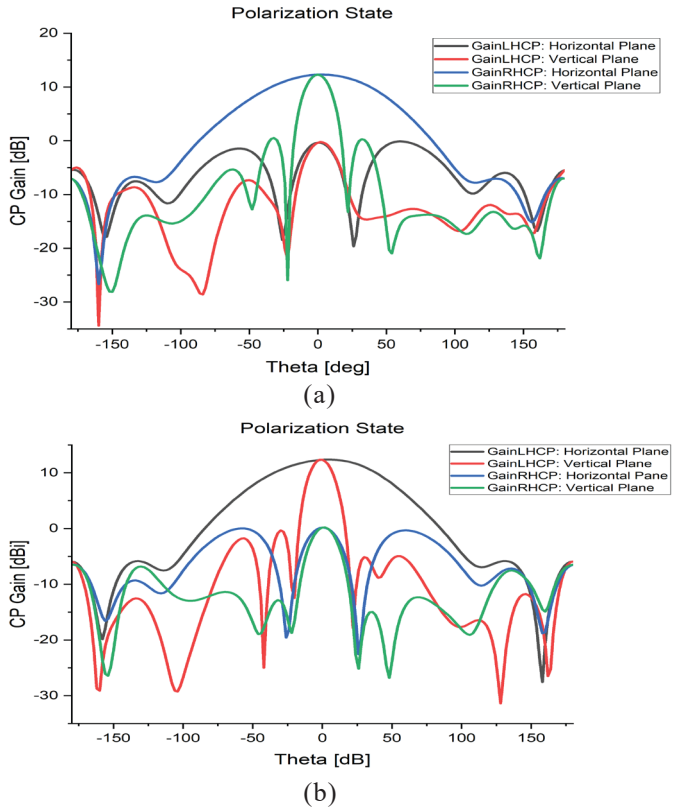

Figure 6. Polarization state graphs of antenna exhibits (a) Right-Handed Circular Polarization (RHCP) when both layers are excited in same phase; and (b) Left-Handed Circular Polarization (LHCP) when both layers are excited in the opposite phase. (All measurements taken at a design frequency of 2.5 GHz).

3.2 Measured Results

A 1×4 polarization agile waveguide slotted array antenna has been fabricated and tested to verify the design. The bottom layer of the antenna is an aluminum WR340 waveguide of cross-section 86.36 mm by 43.18 mm. The total length of the 4-element array is 457.93 mm with a thickness of about 2 mm. The antenna's top layer is a 1.6 mm (approximately 0.06 in) thick Rogers RT/Duroid 5880 substrate. It has been attached to the top of the waveguide with an adhesive layer. The size of the substrate layer is 383.73 mm by 155.13 mm. A corporate power divider network for power feed to the four patch elements has been designed to ensure that all four elements are at the same phase to prevent accidental beam squint. For the experimental setup, the two layers of the antenna have independent connections to the antenna power source (microwave signal generator) using SMA cables and a power splitter. The bottom layer is connected using a coax-to-waveguide connector, while the top layer is connected via a standard SMA connector. Power is fed to the system to ensure zero phase difference between

the two ports. The frequency response of the antenna has been measured using a Bird BN100+ Vector Network Analyzer. Measured v/s simulated return loss is represented in Fig. 7.

Simulation findings show that the antenna's impedance bandwidth is around 30 MHz with a return loss larger than -15 dB. The measured frequency response values are similar to the simulated ones. The pattern of the manufactured antenna was measured at 100 intervals using a Krytar 9000B Power Meter and a Hittite HMC T2100 microwave signal generator (10 MHz- 20 GHz). The measured values of realized gain closely align with the simulated results. Figures 8(a), Fig. 8(b), Fig. 8(c), and Fig. 8(d) show the measured vs. simulated peak realized gain values for the E-plane and H-plane for both Horizontal Linear Polarization and Vertical Linear Polarization states.

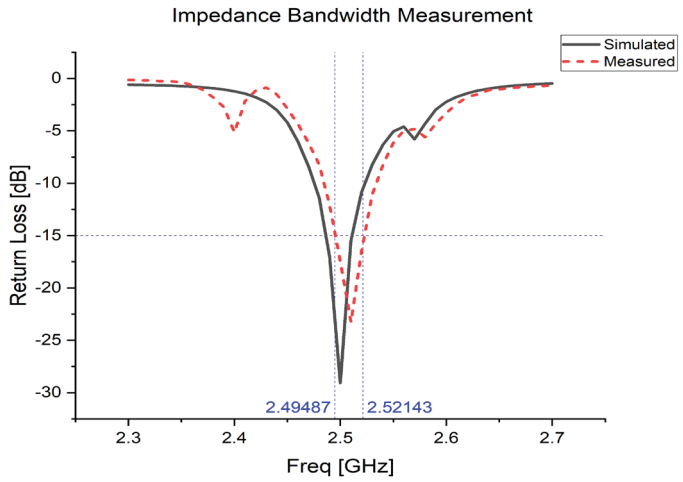

Figure 7. Measured v/s simulated return loss of the proposed antenna.

4. PERFORMANCE BENEFITS OF PROPOSED DESIGN

To demonstrate the advantages of the proposed design, its performance is compared to a parasitic dipole-loaded slotted waveguide antenna array designed and fabricated at the same operating frequency of 2.5 GHz. Once again, the bottom layer comprises an aluminum WR340-based slotted waveguide array antenna. The upper polarizer grid has twelve metallic dipoles printed on a 1.6 mm thick Rogers RT/Duroid 5880 dielectric substrate ($\varepsilon r = 2.2$, $\tan \delta = 0.0009$) without a ground plane. Each slot is paired with a group of three dipoles, spaced 17 mm apart.

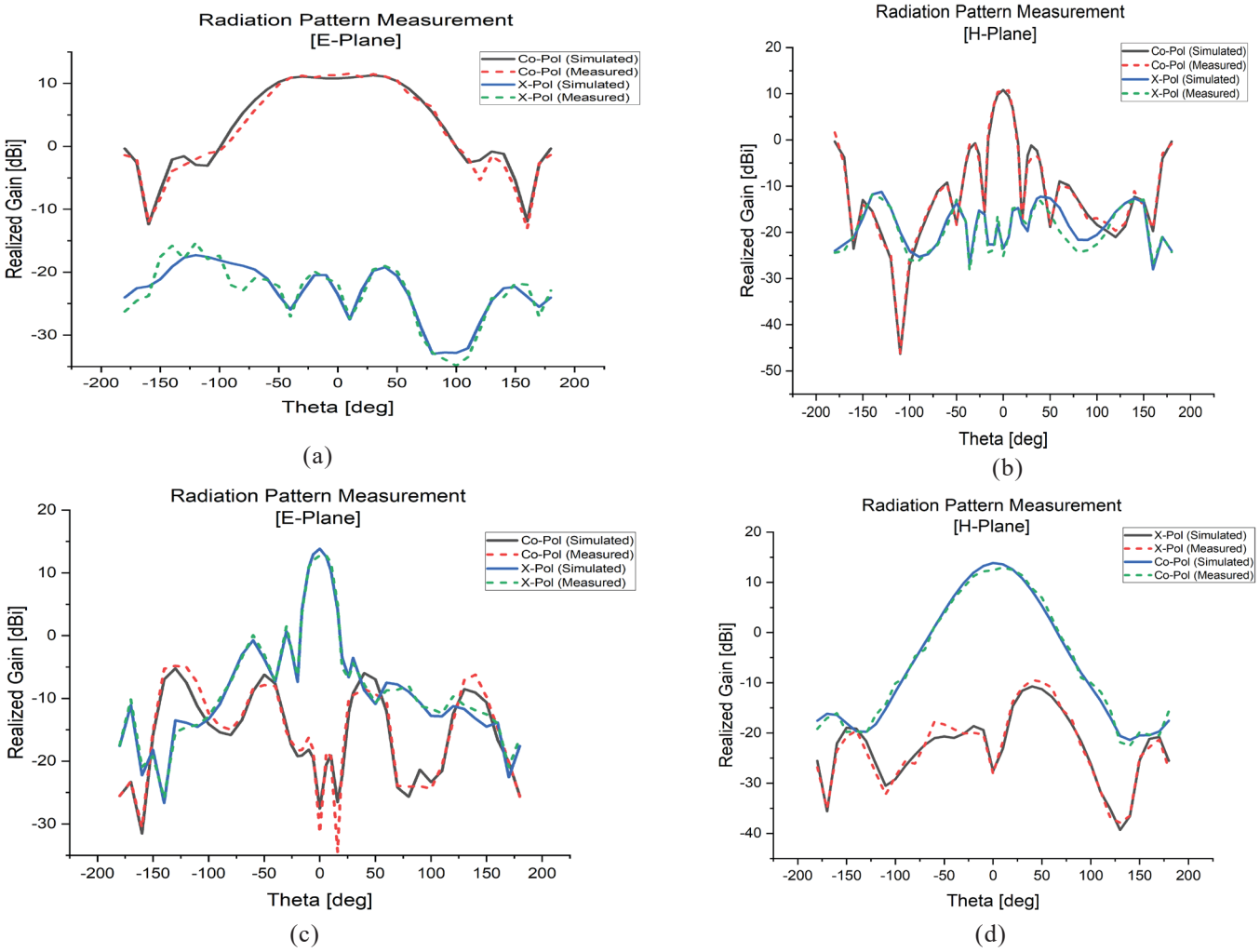

Figure 8. Measured v/s simulated realized gain of the proposed antenna for horizontal polarization state (a) E-Plane cut; and (b) H-Plane cut. The same is also depicted for vertical polarization state; (c) E-Plane cut; and (d) H-Plane cut. (All measurements taken at a design frequency of 2.5GHz).

The schematic diagram and the final fabricated model of the antenna are shown in Fig. 9(a) and Fig. 9(b), respectively.

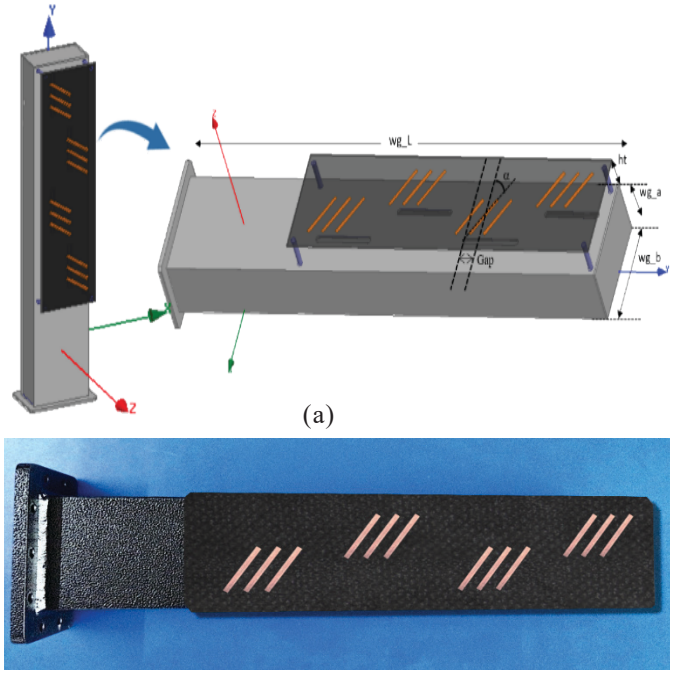

(a)

(b)

Figure 9. (a) Schematic diagram of the slotted waveguide array antenna; and (b) Photograph of the fabricated model of the same antenna.

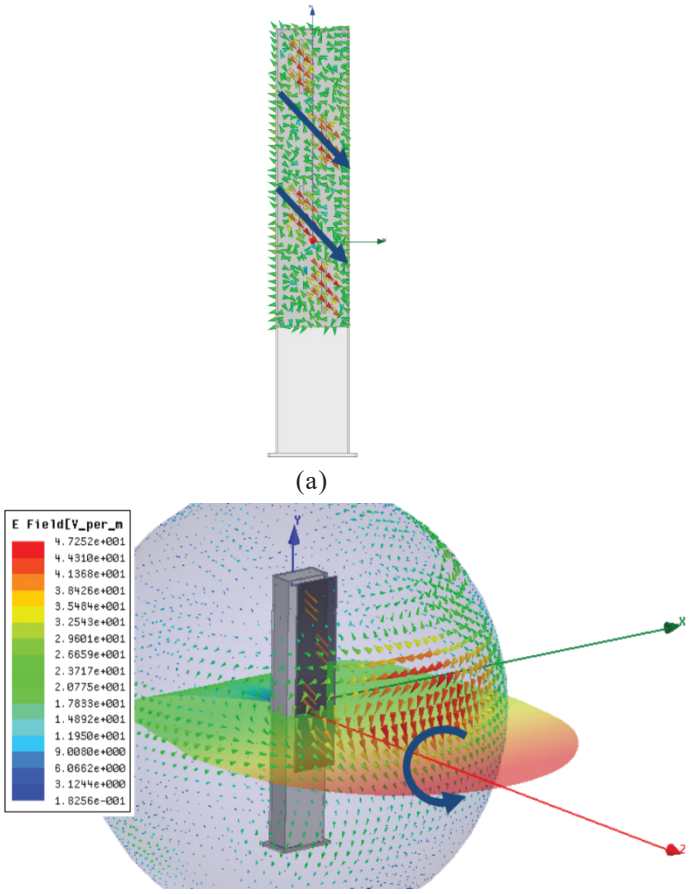

(a)

(b)

Figure 10. (a) Surface current vectors on the radiating face of the antenna; and (b) Electric field vectors at the far field region.

4.1 Performance of Parasitic Dipole-Loaded SWA

Surface current vectors and far-field electric field vectors of the parasitic dipole-loaded SWA are shown in Fig. 10(a) and Fig. 10(b).

Figure 10(b) clearly shows rotational electric field vectors in the far field, indicating circular polarization. This is confirmed by the axial ratio and radiation pattern graphs in Fig. 11(a) and Fig. 11(b). Figure 11(c) verifies that Left-Handed Circular Polarization is generated by the antenna.

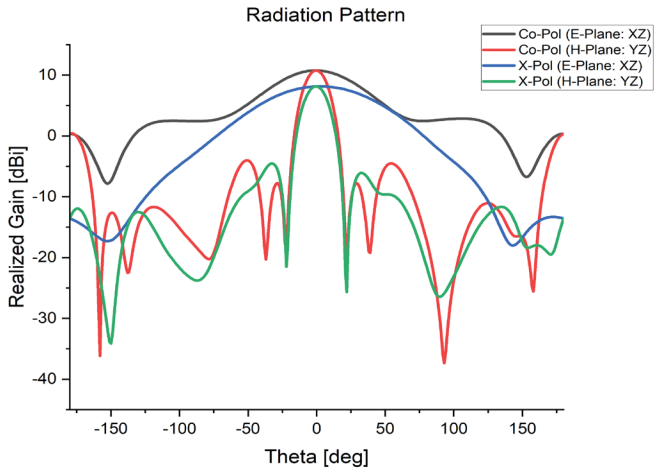

(a)

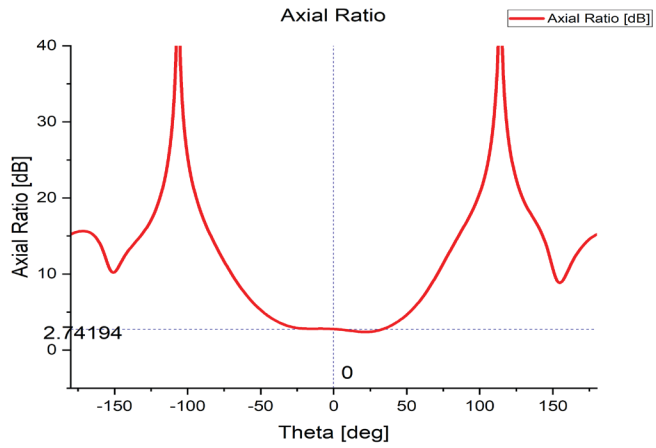

(b)

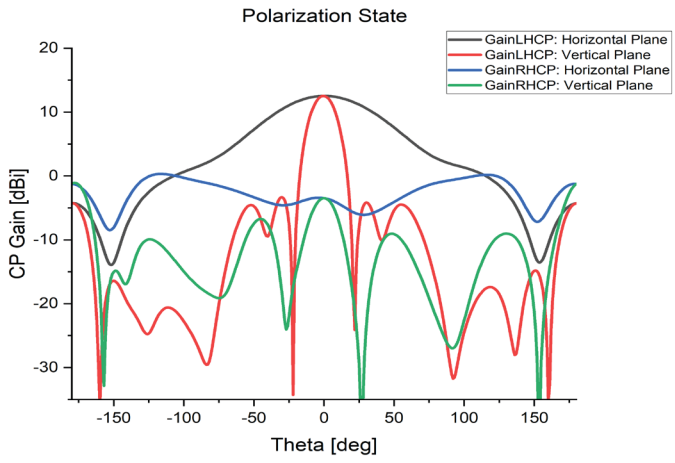

(c)

Figure 11. (a) Graph of radiation pattern; (b) Axial ratio; and (c) Polarization state of the parasitic dipole loaded slotted waveguide array antenna.

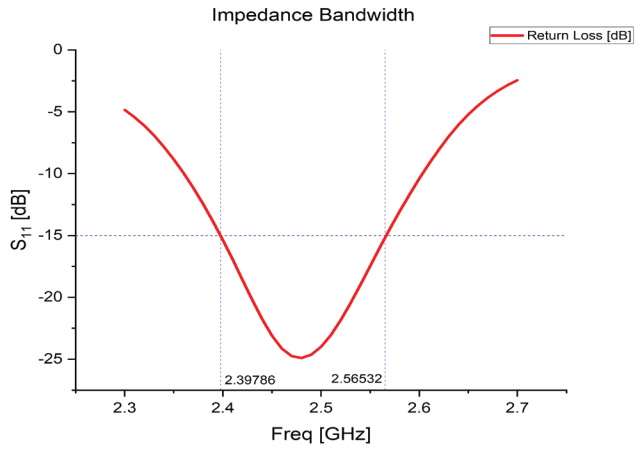

(a)

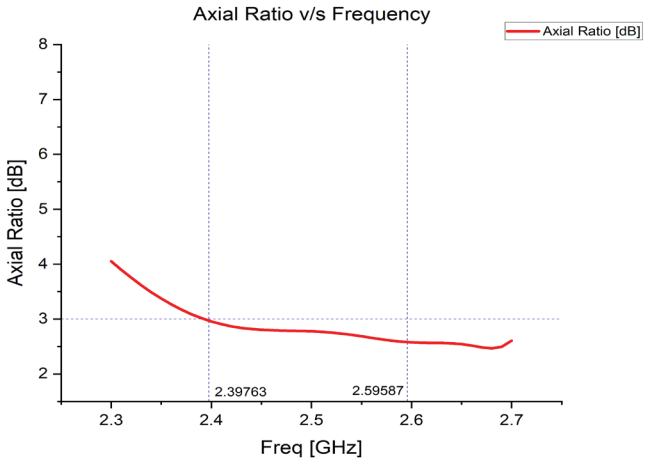

(b)

Figure 12. (a) Graph of impedance bandwidth; and (b) Axial ratio bandwidth of the parasitic dipole loaded slotted waveguide array antenna.

Figure 12(a) & Fig. 12(b) show the frequency response of the designed antenna. The impedance bandwidth of the antenna is 169 MHz. Axial Ratio v/s frequency graph given in Fig. 12(b) shows that circular polarization is maintained throughout the range of the impedance bandwidth.

4.2 Parametric Study

One of the drawbacks of the parasitic dipole loaded slotted waveguide array antenna is the increase in the height profile of the antenna since the polarizing grid needs to be placed at a height of around λ/5 above the radiating slots to achieve proper phase quadrature and generate circular polarized radiation. In the designed antenna, the polarizer grid is at a height of around 25 mm, increasing the height of the original slotted waveguide antenna by about 58 %. The proposed polarization agile antenna uses a new type of polarizer grid where the lateral (instead of vertical) distance between the slot and the patch controls phase quadrature. Hence, the proposed antenna has a much lower height profile. This has been arrived at after a thorough re-evaluation of the polarizer grid with the help of multiple iterations of parametric analysis of the slot-to-patch distance to optimize the positioning of the patch elements in the final design. Some of these results are furnished in this section.

4.2.1 Relationship Between the Height of the Polarizer Grid to Axial Ratio

Figure 13(a) depicts the relationship between the height of the polarizer grid and the axial ratio for the parasitic dipole-loaded slotted waveguide array antenna. It is observed that when the grid is placed immediately above the waveguide antenna, proper phase quadrature is not achieved, resulting in higher axial ratio values. As the height of the polarizer grid is gradually increased, axial ratio progressively decreases, and phase quadrature is eventually achieved at a height of 25 mm with an optimal axial ratio of around 2.7 dB. Figure 13(b) presents the results of a similar study conducted for the proposed antenna. Unlike the parasitic dipole design, there is no discernible relationship between the height of the polarizer grid and the axial ratio in this proposed design.

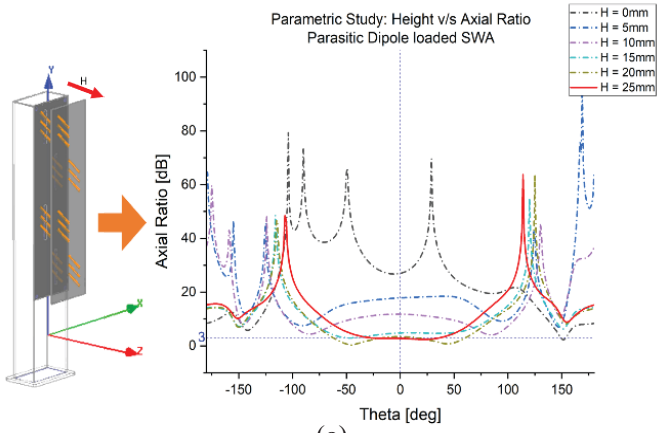

(a)

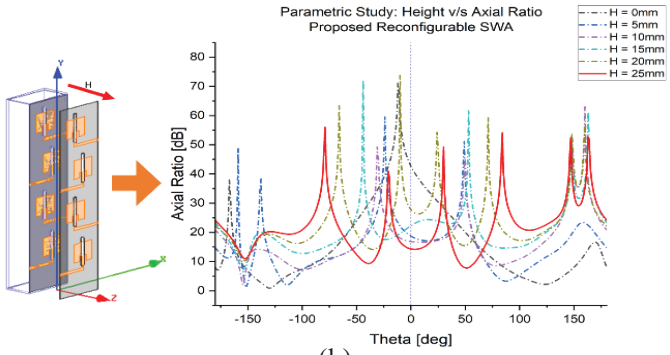

(b)

Figure 13. Parametric study depicting the relationship between the height of the polarizer grid and axial ratio for (a) Parasitic dipole loaded SWA; and (b) Proposed reconfigurable SWA (results considered at 2.5 GHz).

4.2.2 Relationship Between Slot-to-Patch Lateral Distance and Axial Ratio

In the proposed design, the new polarizer grid is positioned directly on top of the slotted waveguide without any vertical separation. A parametric study is carried out on the lateral distance between the patch elements and the radiating slots. The results of the study are given in Fig. 14. The research shows that as the lateral separation between the patch elements and the slots rises, the axial ratio gradually decreases, indicating improved phase quadrature. Optimal phase quadrature is attained at a lateral spacing of about 24 mm, yielding the best axial ratio of 4.8 dB.

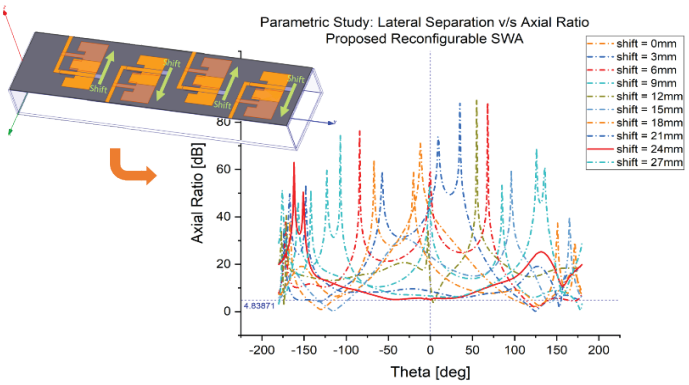

Figure 14. Parametric study depicting the relationship between slot-to-patch lateral distance and axial ratio for the proposed slotted waveguide antenna (results considered at 2.5 GHz).

Table 2 provides a full description of the antenna's design results. At the same polarization state, the results of the parasitic dipole loaded slotted waveguide array and the proposed antenna are nearly identical. The maximum achieved gain for the parasitic dipole loaded antenna at LHCP polarization state is 10.74 dBi, whereas the maximum realized gain for the proposed antenna operating in the same polarization mode is currently 11.66 dBi. Side lobe reduction and cross-polar isolation levels have not deviated much. However, this proposed antenna supports three more polarization states, which were not achievable with the parasitic dipole loaded antenna.

Table 2. Detailed summary of performance (simulation results considered at 2.5 GHz)

Parameters considered	Parasitic dipole loaded SWA	Proposed antena			
Polarization states supported:	1	4			
Polarization state:	LHCP	HLP	VLP	RHCP	LHCP
Realized gain:	10.74 dBi	11.81 dBi	13.84 dBi	11.86 dBi	11.66 dBi
Side lobe reduction:	15.29 dB	11.89 dB	14.49 dB	11.91 dB	14.31 dB
Cross polar isolation:	15.99 dB	34.84 dB	41.42 dB	12.83 dB	12.72 dB
Impedance bandwidth:	169 MHz	32 MHz			

5. CONCLUSIONS

This study presents a polarization-agile waveguide slot array antenna that can electronically switch between four polarization states: horizontal linear polarization, vertical linear polarization, right-handed circular polarization, and left-handed circular polarization. The antenna is intended for S-band radar applications and has been tuned to function at 2.5 GHz. The suggested antenna has two layers: the lower layer is a 4-element waveguide slot array, and the upper layer is a specially constructed actively controlled microstrip patch array. The actual and predicted results agree well, indicating that the proposed antenna module's design process is practical. Results indicate the antenna exhibits a gain of around 11.81 dBi (Horizontal Linear Polarization), 13.84 dBi (Vertical Linear Polarization), 11.86 dBi at RHCP, and 11.66 dBi at LHCP with an axial ratio of about 1.1 dB. The measured impedance bandwidth is around 32 MHz.

Overall, it can be stated that incorporating the active polarizing grid with the waveguide slot array, rather than the passive parasitic dipole-based polarizer, has brought the benefit of polarization diversity as needed. Therefore, this study can be considered as a viable option for developing a highly integrated polarization agile antenna array, specifically in waveguide-based structures for advanced radar applications.

REFERENCES

1. Lee J-S, Pottier E. Polarimetric Radar Imaging: From Basics to Applications. Boca Raton: CRC Press; 2017. doi:10.1201/9781420054989
2. Gao S, Cao Y, Zhang W, Dai Q, Li J, Xu X. Learning feature fusion for target detection based on polarimetric imaging. Appl Opt. 2022;61(7):D15–D21. doi:10.1364/AO.441183
3. Luzi G, Dematteis N. Ku band terrestrial radar observations by means of circular polarized antennas. Remote Sens. 2019;11(3):270. doi:10.3390/rs11030270
4. Yuan M, Zhang L, Wang Y, Han C. Polarimetric range extended target detection via adaptive range weighted feature extraction. Remote Sens. 2023;15:2929. doi:10.3390/rs15112929
5. Alhuwaimel, S. Fully polarimetric slotted waveguide antenna array design. Dept. Electronic and Electrical Eng., University College London, UK, 2018. (PhD Thesis).
6. Chakrabarti M, Gangopadhyaya M, Chattopadhyay A. Slotted waveguide antenna for microwave remote sensing applications. In: 2023 IEEE Devices for Integrated Circuit (DevIC); 2023 Apr 14-15; Kalyani, India. p. 42–7. doi:10.1109/DevIC57758.2023.10134877
7. Shah M, Cheema HM, Abbasi QH. Substrate integrated waveguide antenna system for 5G in-band full duplex applications. Electronics. 2021;10(20):2456. doi:10.3390/electronics10202456
8. Trinh TV, Park J, Song CM, Song S, Hwang KC. A 3-D metal-printed dual-polarized ridged waveguide slot array antenna for X-band applications. Appl Sci. 2023;13(8):4996. doi:10.3390/app13084996
9. Chen M, Fang XC, Wang W, Zhang TH, Huang GL. Dual-band dual-polarized waveguide slot antenna for SAR applications. IEEE Antennas Wirel Propag Lett. 2020;19(10):1719–23. doi:10.1109/LAWP.2020.3014878
10. Aboserwal N, Salazar-Cerreno JL, Qamar Z. An ultra-compact X-band dual-polarized slotted waveguide array unit cell for large E-scanning radar systems. IEEE Access.

2020;8:210651–62.
doi:10.1109/ACCESS.2020.3038485
11. Wang W, Jin J, Liang XL, Zhang ZH. Broadband dual polarized waveguide slotted antenna array. In: 2006 IEEE Antennas and Propagation Society International Symposium; 2006 Jul 9-14; Albuquerque, NM. p. 2237–40.
doi:10.1109/RADAR.2006.1435907
12. Herranz-Herruzo JI, Ferrando-Rocher M, Valero-Nogueira A, Bernardo-Clemente B. Wideband circularly polarized mm-wave array antenna using H-shaped low-axial-ratio apertures. IEEE Trans Antennas Propag. 2023;71(5):4564–9.
doi:10.1109/TAP.2023.3253209
13. Jing X, Zhu Z, Wang Y, Peng Y. Waveguide slotted array antenna for circularly polarized radiation field. In: 16th International Conference on Electronic Packaging Technology (ICEPT); 2015 Aug 11-14; Changsha, China.
doi:10.1109/ICEPT.2005.7236841
14. Montisci G. Design of circularly polarized waveguide slot linear arrays. IEEE Trans Antennas Propag. 2006;54(10):3025–9.
doi:10.1109/TAP.2006.882201
15. Ayoub FN, Tawk Y, Ardelean E, Costantine J, Lane SA, Christodoulou CG. Cross-slotted waveguide array with dual circularly polarized radiation at W-band. IEEE Trans Antennas Propag. 2022;70(1):268–77.
doi:10.1109/TAP.2021.3090863
16. Chatterjee S, Majumder A. Design of circularly polarized waveguide crossed slotted array antenna at Ka band. In: 2015 International Conference on Microwave and Photonics (ICMAP); 2015 Dec 4-6; Dhanbad, India. p. 1–2.
doi:10.1109/ICMAP.2015.7408714
17. Kazemi R, Yang S, Suleiman SH, Fathy AE. Design procedure for compact dual-circularly polarized slotted substrate integrated waveguide antenna arrays. IEEE Trans Antennas Propag. 2019;67(6):3839–52.
doi:10.1109/TAP.2019.2905682
18. Ma Y, Hu J, Zhang Y, Li L, Liu L. Design of circularly polarized slotted waveguide antenna for SAR application. In: 2018 China International SAR Symposium (CISS); 2018 Oct 10-12; Shanghai, China. p. 1–3.
doi:10.1109/SARS.2018.8552005
19. Yoon SJ, Choi JH. A Ka-band circular polarized waveguide slot antenna with a cross iris. Appl Sci. 2020;10(19):6994.
doi:10.3390/app10196994
20. Wu X, Yang F, Xu F, Zhou J. Circularly polarized waveguide antenna with dual pairs of radiation slots at Ka-band. IEEE Antennas Wirel Propag Lett. 2017;16:2947–50.
doi:10.1109/LAWP.2017.2755022
21. Yoon SJ, Choi JH. A Ka-band circular polarized waveguide slot antenna with a cross iris. Appl Sci. 2020;10(19):6994.
doi:10.3390/app10196994
22. Kai Z, Jianying L, Yi Y, Rui X. A novel design of circularly polarized waveguide antenna. In: 2014 3rd Asia-Pacific Conference on Antennas and Propagation (APCAP); 2014 Jul 26-29; Harbin, China. p. 130–3.
doi:10.1109/APCAP.2014.6992431
23. Herranz-Herruzo JI, et al. Low cost switchable RHCP/LHCP antenna for SOTM applications in Ka-band. In: 2015 9th European Conference on Antennas and Propagation (EuCAP); 2015 Apr 13-17; Lisbon, Portugal. p. 1–4.
24. Gonzalez-Ovejero D, Herranz-Herruzo JI, Valero-Nogueira A, Balbastre-Tejedor JV. Design of radome-covered slot-array antennas loaded with parasitic dipoles for circular polarization at Ka-band. In: The Second European Conference on Antennas and Propagation (EuCAP); 2007 Nov 11-16; Edinburgh, UK. p. 1–6.
doi:10.1049/ic.2007.0866
25. Ferrando-Rocher M, Herranz-Herruzo JI, Valero-Nogueira A, Rodrigo VM. Circularly polarized slotted waveguide array with improved axial ratio performance. IEEE Trans Antennas Propag. 2016;64(9):4144–8.
doi:10.1109/TAP.2016.2586492
26. Stevenson AF. Theory of slots in rectangular waveguides. J Appl Phys. 1948;19(1):24–38.
doi:10.1063/1.1697868
27. Oliner AA. The impedance properties of narrow radiating slots in the broad face of rectangular waveguide: Part I & II. IRE Trans Antennas Propag. 1957;5(1):4–20.
doi:10.1109/TAP.1957.1144488
28. Watson WH. Resonant slots. J Inst Electr Eng Part IIIA Radiolocation. 1946;93(4):747–77.
29. Stegen RJ. Slot radiators and arrays at X-band. IRE Prof Group Antennas Propag. 1952;1(1):62–84.
doi:10.1109/TPGAP.1952.6366355
30. Johnson RC, Jasik H. Antenna Engineering Handbook. 3rd ed. New York: McGraw-Hill; 1993.

CONTRIBUTORS

Mr Mandar Chakrabarti obtained MTech in Radio Physics & Electronics from Calcutta University with specialization in Microwave Engineering & Space Science. He is working as an Assistant Professor in the Department of Electronics & Communication Engineering at University of Engineering & Management, Kolkata. His research interests include: Microwave and millimeter wave antennas, slotted waveguide arrays, remote sensing and GNSS technology.
In the current study: He conducted the simulation of the proposed antenna, meticulously collected, analyzed, interpreted, and discussed results, and wrote the manuscript.

Dr Abir Chattopadhyay obtained his PhD from Jadavpur University in the field of Microelectronics. His research interest include: Solid state electronics, microelectronics, optical communication and wireless sensor technology.
In the current study: He proposed the design of the antenna and its underlying theory.

Dr Malay Gangopadhyaya obtained PhD from Jadavpur University. His research interests include: Electromagnetics and antenna design.
In the current study: He helped perform all measurements of the fabricated antenna and discussed the results.

Dr Ayan Chatterjee obtained PhD in Microwave Engineering from IIEST, Shibpur. He is working as an Associate Professor in the Department of ECE at University of Engineering and Management, Kolkata. His research interests include: Frequency selective surfaces, metamaterial inspired surfaces, wideband antennas.
In the current study: He was involved in preparing the manuscript as well as revision of the manuscript as per reviewer comments.

Dr Kabita Purkait obtained PhD from Calcutta University. She is working as Associate professor in Deptt. of Electronics and Communication Engineering in Kalyani Govt. Engineering College. Her present interest is in the development of microwave scanner and subsequent reconstruction algorithm in microwave tomography.
In the current study: She helped with the fabrication of the proposed antenna.